Flows over two-dimensional isolated mountains

Earlier, we obtained mountain wave solution forced by a sinusoidal orography. Of course, real orography is never truly sinusoidal. However, one can always perform Fourier transform on the real orography, therefore any orography can be considered summation of many sinusoidal modes or wave components.

When the orography is low, the wave solutions are nearly linear, therefore the total solution is sum of all forced waves.

Let $\hat{w}$ be the amplitude of the wave component with wavenumber *k*, Eq.(13) we obtained earlier is

$$\hat{w}_{zz} + (l^2 - k^2)\hat{w} = 0 . \qquad (37)$$

The Fourier transform of the linear lower boundary condition is

$$\hat{w}(k, z = 0) = ikU\,\hat{h}(k) . \qquad (38)$$

where $\hat{h}(k)$ is the amplitude of Fourier component of orography with wavenumber *k*.

For constant Scorer parameter, the solution we obtained earlier for the wave amplitude can be written into two parts,

$$\hat{w}(k, z) = \hat{w}(k,0)\, e^{i\sqrt{l^2 - k^2}\, z} \quad \text{for } l^2 > k^2 \text{ and} \qquad (39a)$$

$$\hat{w}(k, z) = \hat{w}(k,0)\, e^{-\sqrt{k^2 - l^2}\, z} \quad \text{for } l^2 < k^2 . \qquad (39b)$$

Taking the inverse one-sided Fourier transform of (39) yields the solution in the physical space,

$$w'(x,z) = 2\,\mathrm{Re}\left[\int_0^l ikU\ \hat{h}(k)\ e^{i\sqrt{l^2-k^2}z} e^{ikx} dk + \int_l^\infty ikU\ \hat{h}(k)\ e^{-\sqrt{k^2-l^2}z} e^{ikx} dk\right], \qquad (40)$$

which is basically the summation of all wave components.

The first integration represents the upward propagating wave.

The second integration represents the evanescent waves.

For simplicity, let us consider a bell-shaped mountain mountain profile,

$$h(x) = \frac{h_m a^2}{x^2 + a^2}, \qquad (41)$$

where h_m is the mountain height and a is the half-width. The mountain peak is at x=0.

The one-sided Fourier transform of this mountain profile is in a simple form,

$$\hat{h}(k) = \frac{h_m a}{2} e^{-ka}, \quad \text{for } k > 0. \qquad (42)$$

This $\hat{h}(k)$ is plugged into (41) to obtained the actual solution of *w'*. For this bell shaped mountained, the characteristic wavenumber of forcing is $k = 1/a$.

Cases to consider:

First case: $l^2 << k^2$ **(i.e.,** $al << 1$ **or** $Na << U$ **).**

We assumed that *U* and *N* are constant with height.

In this case, the second integral on the right hand side of (40) can be neglected, and the final solutions are

$$w'(x,z) \approx 2\,\mathrm{Re}\left[U\int_0^\infty ik\left(\frac{h_m a}{2}\right)e^{-ka}\ e^{-kz}e^{ikx}dk\right]. \qquad (43)$$

$$\eta(x,z) = h_m a\,\mathrm{Re}\int_0^\infty e^{-k(z+a-ix)}dk = \frac{h_m a(z+a)}{x^2+(z+a)^2}. \qquad (44)$$

$\eta(x,z)$ is the vertical displacement of the streamline from the far updream level.

Therefore, similar to the sinusoidal mountain case, the flow pattern is symmetric with respect to the center of the mountain ridge ($x = 0$). However, the amplitude decreases with height linearly, instead of exponentially. The flow pattern is depicted below.

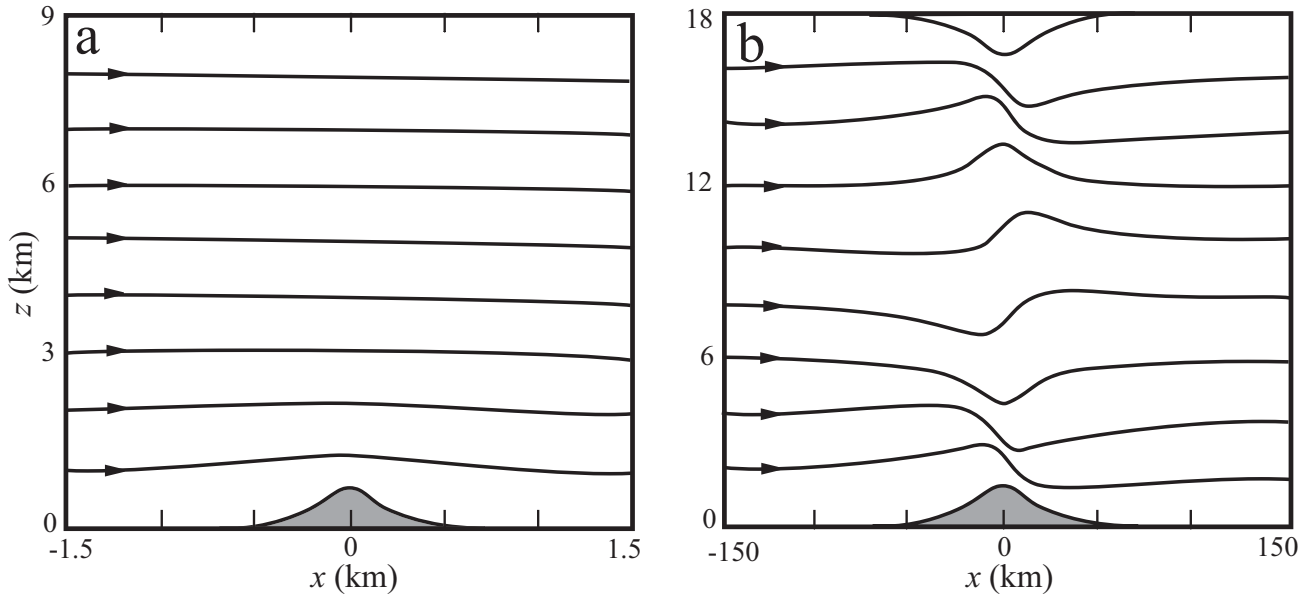

Fig. 5.3: Streamlines of steady state flow over an isolated, bell-shaped mountain when (a) $l^2 << k^2$ (or $Na << U$), where a is the half-width of the mountain, or (b) $l^2 >> k^2$ (or $Na >> U$). (Adapted after Durran 1990)

Second case: $l^2 >> k^2$ **(i.e.,** $al >> 1$ **or** $Na >> U$**).**

In this case, the first integral on the right hand side of (40) can be neglected, and the final solutions are

$$w'(x,z) \approx 2\,\mathrm{Re}\left[U\int_0^\infty ik\hat{h}(k)e^{ilz}e^{ikx}dk\right] = 2\,\mathrm{Re}\left[U\int_0^\infty ik\left(\frac{h_m a}{2}\right)e^{-ka}e^{ilz}e^{ikx}dk\right]. \qquad (45)$$

Similarly, the vertical displacement can be obtained,

$$\eta(x,z) = 2\,\mathrm{Re}\int_0^\infty \frac{h_m a}{2} e^{-ka} e^{i(kx+lz)} dk = \frac{h_m a(a\cos lz - x\sin lz)}{x^2 + a^2}\,. \qquad (46)$$

This type of flow is characterized as a hydrostatic mountain wave.

The disturbance confines itself over the mountain in horizontal, but repeats itself in vertical with a wavelength of $2\pi U / N$.

If the density effect is included, the above solution becomes

$$\eta(x,z) = \left(\frac{\rho_s}{\rho(z)}\right)^{1/2} \left[\frac{h_m a(a\cos lz - x\sin lz)}{x^2 + a^2}\right], \qquad (47)$$

where ρ_s is the air density near surface.

It says that the wave amplitude will increase with a decreased air density of the basic flow.

Third case, $l^2 \approx k^2$ **(i.e.,** $al \approx 1$ **or** $Na \approx U$ **)**

In this case, all terms of the vertical momentum equation, (40) are equally important.

Both asymptotic methods and numerical methods have been applied to solve the problem. The solution looks like:

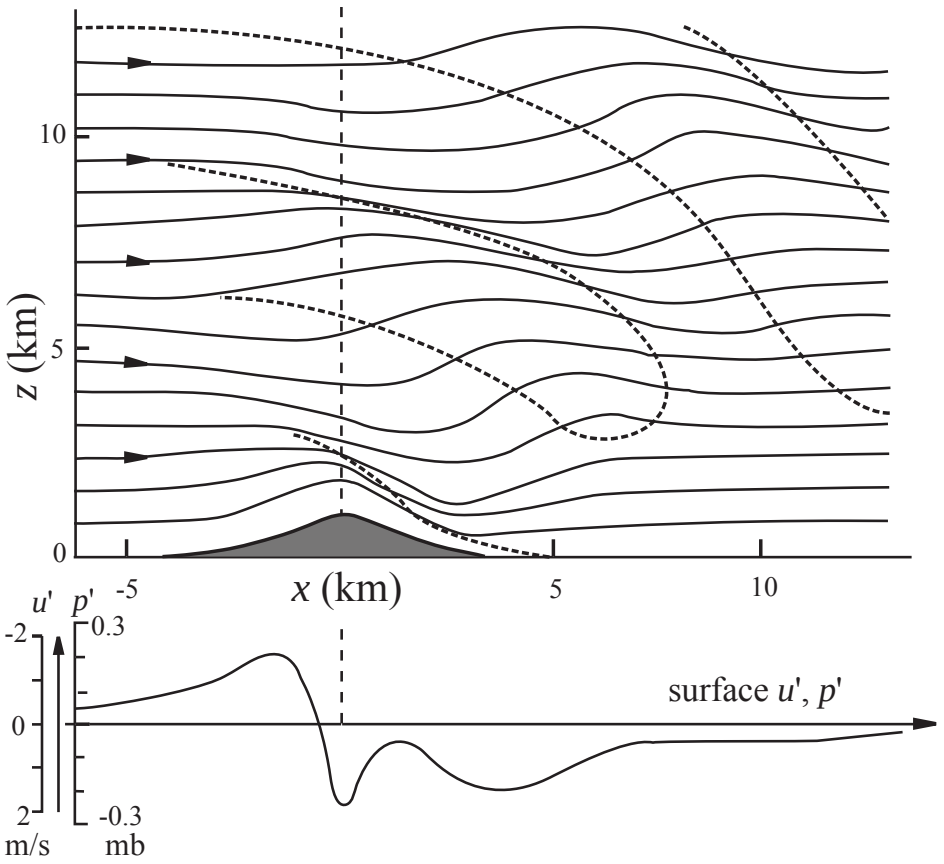

Flow over a two-dimensional ridge of intermediate width ($l^2 \approx k^2$, or $al = Na/U = 1$) where the buoyancy force is important, but not so dominant that the flow is hydrostatic. The zero phase lines are denoted by dotted curves. The waves on the lee aloft are the *dispersive tail* of the nonhydrostatic waves ($k < l$, but not $k << l$). The flow and orographic parameters are: U = 10 ms^{-1}, N = 0.01 s^{-1}, h_m = 1 km, and a = 1 km. (Adapted after Queney 1948)

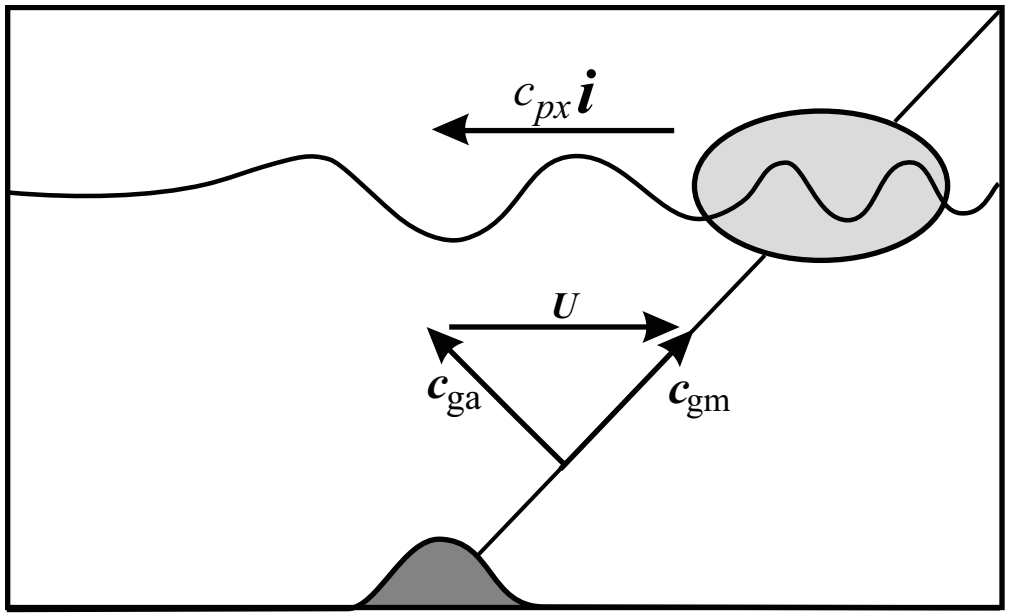

A schematic illustrating the relationship among the group velocity with respect to (w.r.t) to the air ($\boldsymbol{c}_{\mathrm{ga}}$), group velocity w.r.t. to the mountain ($\boldsymbol{c}_{\mathrm{gm}}$), horizontal phase speed ($c_{px}\boldsymbol{i}$) and the basic wind. The horizontal phase speed of the wave is exactly equal and opposite to the basic wind speed. The wave energy propagates upward and upstream relative to the air, but is advected downstream by the basic wind. The energy associated with the mountain waves propagates upward and downstream relative to the mountain. (Adapted after Smith 1979)

Trapped lee waves

One of the most prominent features of mountain waves is the long train of wave clouds over the lee of mountain ridges in the lower atmosphere. This type of wave differs from the dispersive tails shown earlier for the $l^2 \approx k^2$ case in that it is located in the lower atmosphere and there is no vertical phase tilt.

This type of trapped lee waves occur when the Scorer parameter decreases rapidly with height (Scorer 1949).

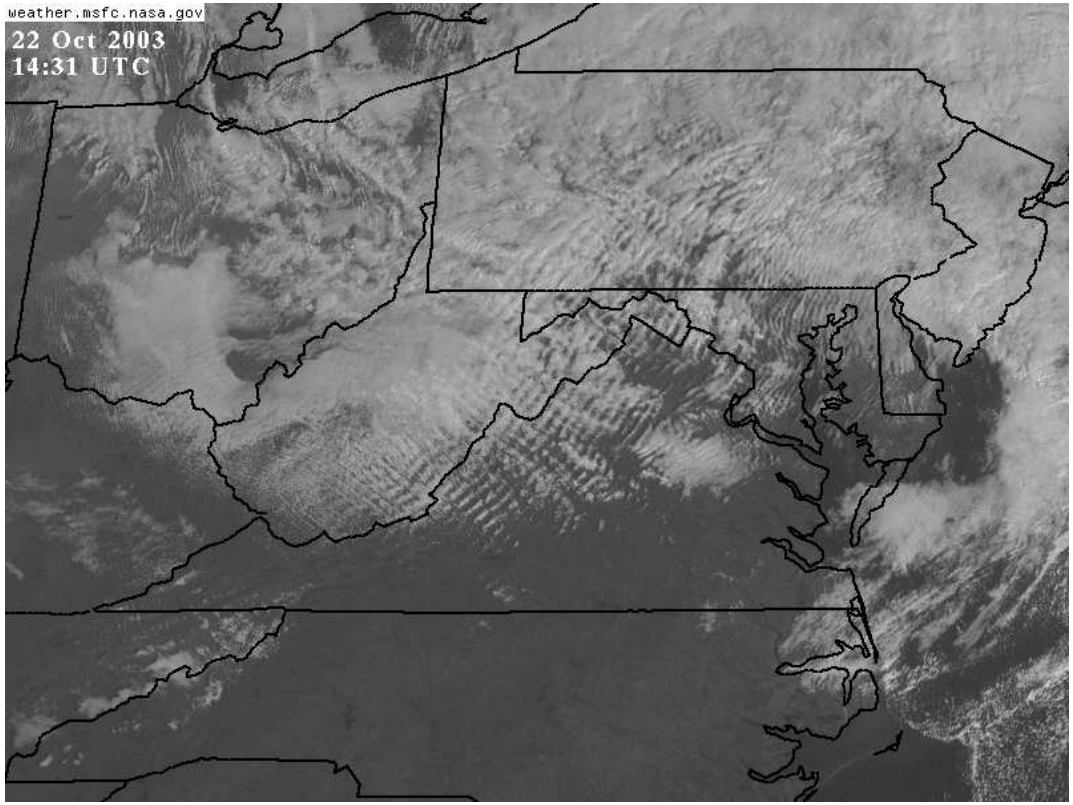

Satellite imagery for lee wave clouds observed at 1431 UTC, 22 October 2003, over western Virginia. Clouds originate at the Appalachian Mountains. (Courtesy of NASA)

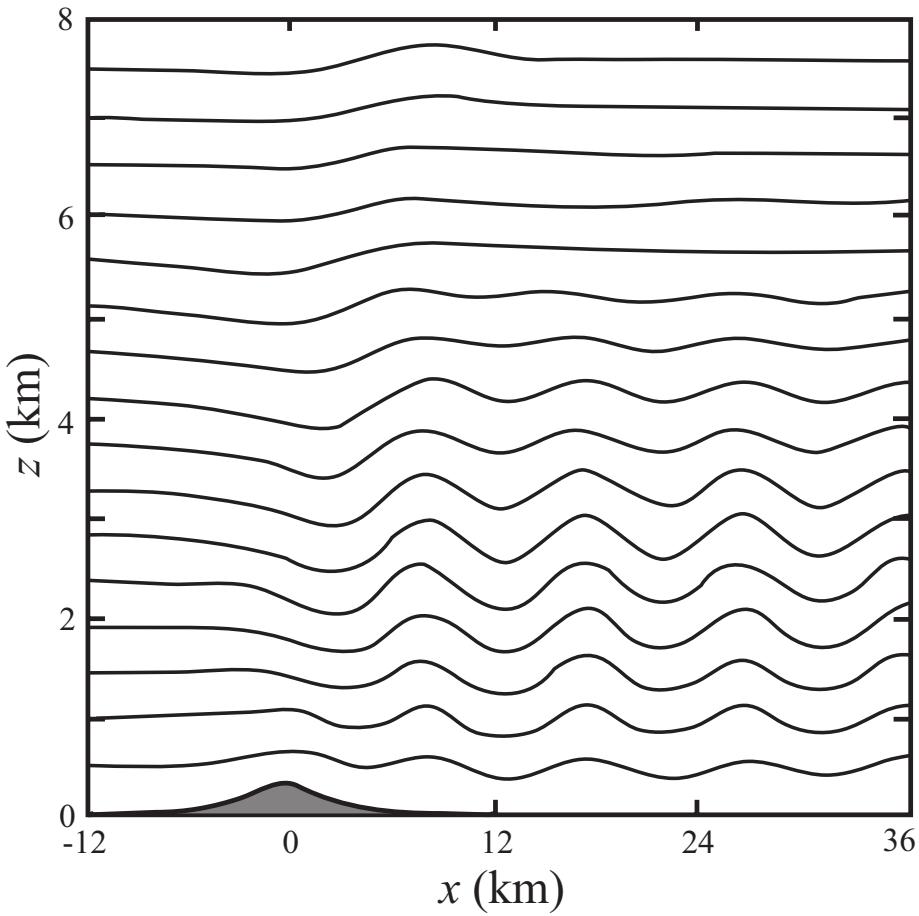

Figure. Lee waves simulated by a nonlinear numerical model for a two-layer airflow over a bell-shaped mountain. Displayed are (a) the quasi-steady state streamlines and (b) the vertical profiles of temperature and wind speed (solid lines) used for (a). (Adapted after Durran 1986b)

- Due to the co-existence of the upward propagating waves and downward propagating waves, there exists no phase tilt in the lee waves.

- Once lee waves form, regions of reversed cross-mountain winds near the surface beneath the crests of the lee waves may develop due to the presence of a reversed pressure gradient force.

- In the presence of surface friction, a sheet of vorticity parallel to the mountain range forms along the lee slopes, which originates in the region of high shear within the boundary layer.

- The vortex sheet separates from the surface, ascends into the crest of the first lee wave, and remains aloft as it is advected downstream by the undulating flow in the lee waves (Doyle and Durran 2004).

- The vortex with recirculated air is known as *rotor* and the process that forms it is known as *boundary layer separation*.

- These rotors are often observed to the lee of steep mountain ranges such as over the Owens Valley, California, on the eastern slope of Sierra Nevada (e.g., Grubišić and Lewis 2004).

- Occasionally, a turbulent, altocumulus cloud forms with the rotor and is referred to as *rotor cloud*.

Nonlinear flows over two-dimensional mountains

- The linear dynamics of mountain waves over 2d ridges are fundamentally understood.
- Linear theory, however, begins to break down when the perturbation velocity (*u'*) becomes large compared with the basic flow (*U*) in some regions, so that the flow becomes stagnant.
- This happens when the mountain becomes very high, the basic flow becomes very slow, or the stratification becomes very strong.
- In other words, flow becomes more nonlinear when the *Froude number*, $F = U / Nh$, becomes small.
- For simplicity, the mountain height is denoted by h . Thus, in order to fully understand the dynamics of nonlinear phenomena, such as upstream blocking, wave breaking, severe downslope winds and lee vortices, we need to take a nonlinear approach.
- Nonlinear response of a continuously stratified flow over a mountain is very complicated since the nonlinearity may come from the basic flow characteristics, the mountain height, or the transient behavior of the internal flow, such as wave steepening.

Long (1953) derived the governing equation for the finite-amplitude, steady state, two-dimensional, inviscid, continuously and stably stratified flow and obtained an equation for vertical displacement of streamline from its far upstream δ that looks essentially the same as the equation for w' that we derived earlier for linear waves:

$$\nabla^2 \delta + l^2 \delta = 0, \qquad (48)$$

where $l = N / U$ is the Scorer parameter of the basic flow far upstream.

The main difference from the linear problem is that nonlinear lower boundary condition has to be used to represent the finite-amplitude mountain:

$$\delta(x,z) = h(x) \quad \text{at } z = h(x). \qquad (49)$$

The nonlinear lower boundary condition is applied on the mountain surface, instead of approximately applied at $z = 0$ as in the linear lower boundary condition.

The general solution to (49) is actually similar to the linear solutions we obtained earlier.

Next figure shows streamlines of analytical solutions for flow over a semi-circle obstacle for the nondimensional mountain heights Nh/U = 0.5, 1.0, 1.27, and 1.5.

The reciprocal of the Froude number (U/Nh) is often called the nondimensional mountain height which is a measure of the nonlinearity of the continuously stratified flow.

When Nh/U is small, such as $Nh/U = 0.5$, the flow is more linear.

When Nh/U increases to 1.27, the flow becomes more nonlinear and its streamlines become vertical at the first level of wave steepening.

For flow with $Nh/U > 1.27$, the flow becomes statically and dynamically (shear) unstable.

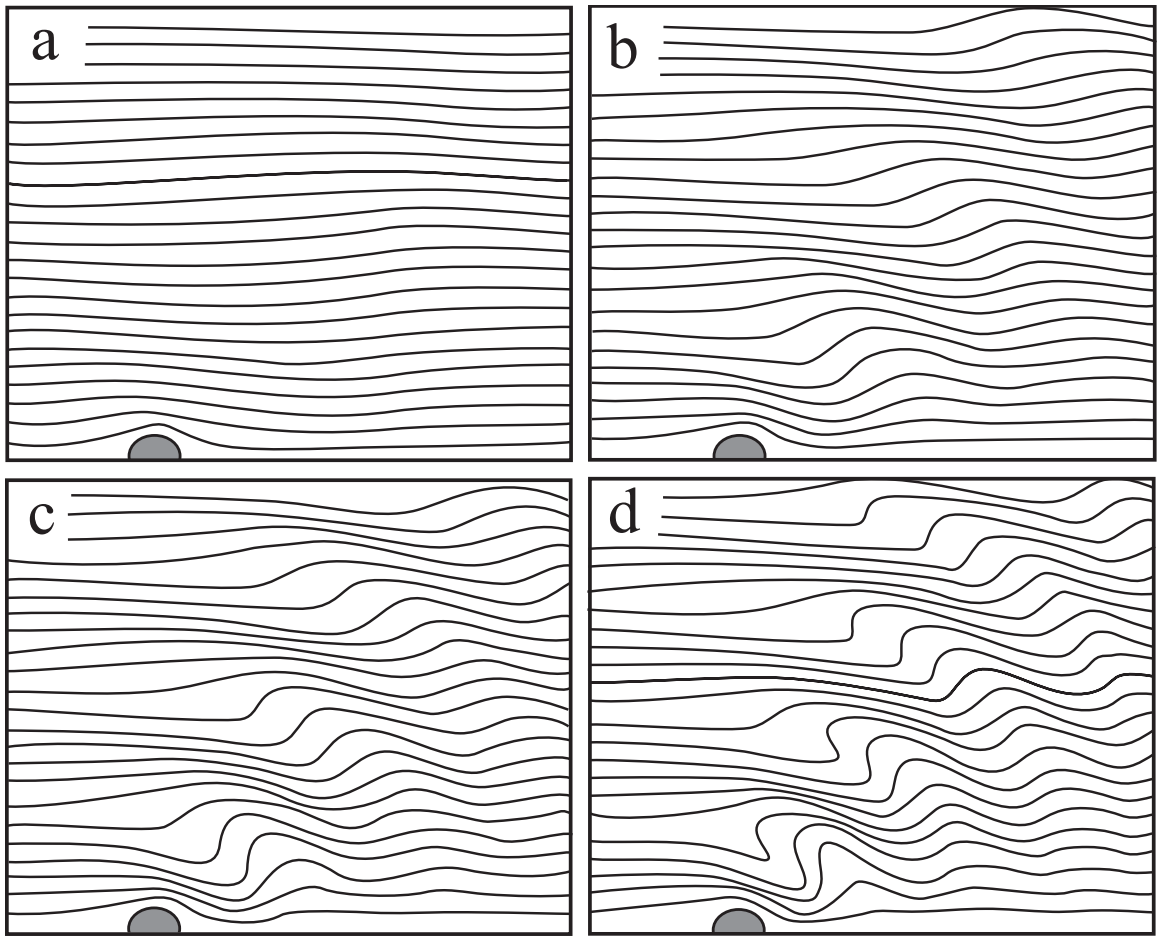

Streamlines of Long's model solutions for uniform flow over a semi-circle obstacle with Nh/U = (a) 0.5, (b) 1.0, (c) 1.27, and (d) 1.5. Note that the streamlines become vertical in (c) and overturn in (d). (Adapted after Miles 1968)

This mountain is rather narrow, compared to the vertical scale height $1/l$, with l being the Score parameter. The the waves are non-hydrostatic and there is a downstream wave train at the upper levels.

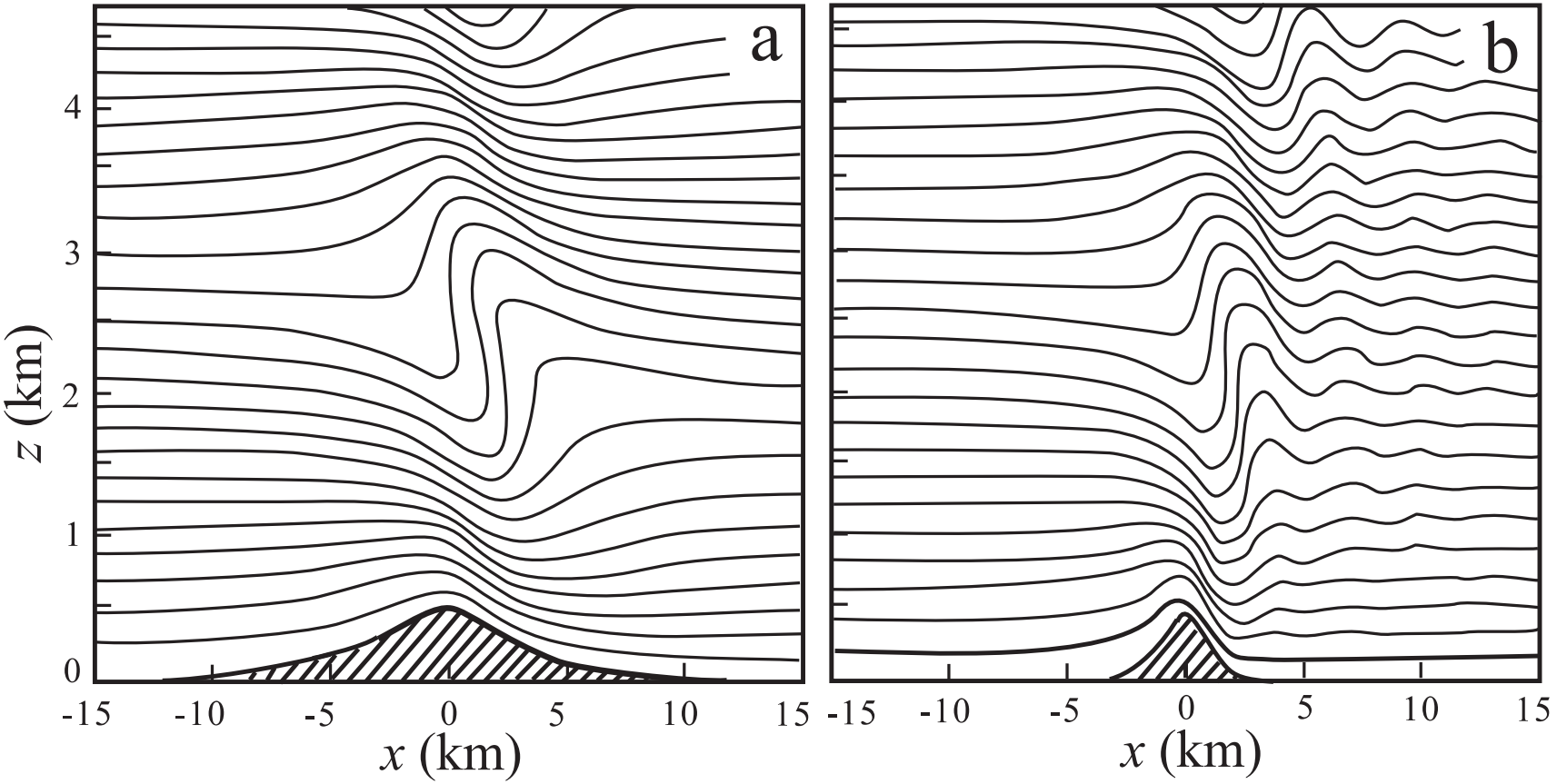

Figure (a) Streamlines for Long's model solution over a bell-shaped mountain with U = 5 ms^{-1}, N = 0.01 s^{-1}, h_m = 500 m (Nh/U =1, l =N/U=0.002 m^{-1}) and a = 3 km; and (b) same as (a) except with a = 1 km. Note that the dispersive tail of the nonhydrostatic waves is present in the narrower mountain (case (b)). In both cases, the mountain is height enough to force over turning of the streamlines above the mountain, also that of wider mountain is steep, because there is no downstream dispersion of wave energy.

Generation of severe downslope winds

Severe downslope winds over the lee of a mountain ridge have been observed in various places around the world, such as the *chinook* over the Rocky Mountains, *foehn* over the Alps.

One well-known event is the 11 January 1972 windstorm occurred in Boulder, Colorado, and which reached a peak wind gust as high as 60 ms^{-1} and produced severe damage in the Boulder, Colorado area.

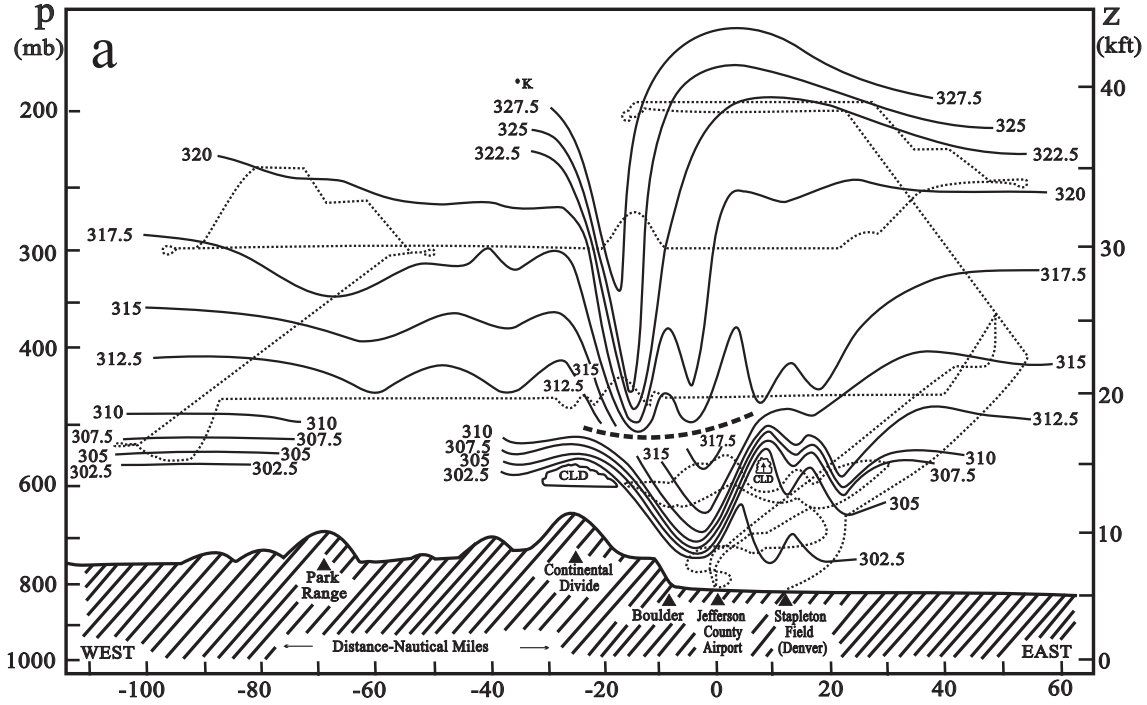

Figure. Analysis of potential temperature from aircraft flight data and rawinsondes for the 11 January 1972 Boulder windstorm. The bold dashed line separates data taken from the Queen Air aircraft (before 2200 UTC) and from the Saberliner aircraft (after 0000 UTC) (Adapted after Klemp and Lilly 1975).

The basic dynamics of the severe downslope wind can be understood from the following two major theories: (a) *resonant amplification theory* (Clark and Peltier 1984), and (b) *hydraulic theory* (Smith 1985), along with later studies on the effects of instabilities, wave ducting, nonlinearity, and upstream flow blocking.

Resonant amplification theory

Idealized nonlinear numerical experiments indicate that a high-drag (severe-wind) state occurs after an upward propagating mountain wave breaks above a mountain.

The wave-breaking region is characterized by strong turbulent mixing , with a local wind reversal on top of it.

Wind reversal level coincides with the critical level for a stationary mountain wave, and thus is also referred to as the *wave-induced critical level*.

Waves can not propagation through the critical level and are reflected downwards.

The wave breaking region aloft acts as an internal boundary which reflects the upward propagating waves back to the ground and produces a high-drag state through partial resonance with the upward propagating mountain waves.

When the basic-flow critical level is located at a nondimensional height of $z_i/\lambda_z = 3/4 + n$ (n is an integer, z_i is a prescribed critical level height, $\lambda_z = 2\pi U_o / N$) above the surface, nonlinear resonant amplification occurs between the upward propagating waves generated by the mountain and the downward propagating waves reflected from the critical level.

On the other hand, when the basic flow critical level is located at a nondimensional height off $z_i/\lambda_z = 3/4 + n$, such as 1.15, there is no wave resonance and no severe downslope winds generated.

Because the severe downslope winds are developed by resonance between upward and downward waves, this mechanism is referred to as the *resonant amplification mechanism*.

For the above reasons, the vertical structure of the atmosphere, particularly in terms of the Score parameter, as it determines the vertical wavelength, is most important for the on set of resonant response, given sufficiently strong orographic forcing to cause wave breaking or

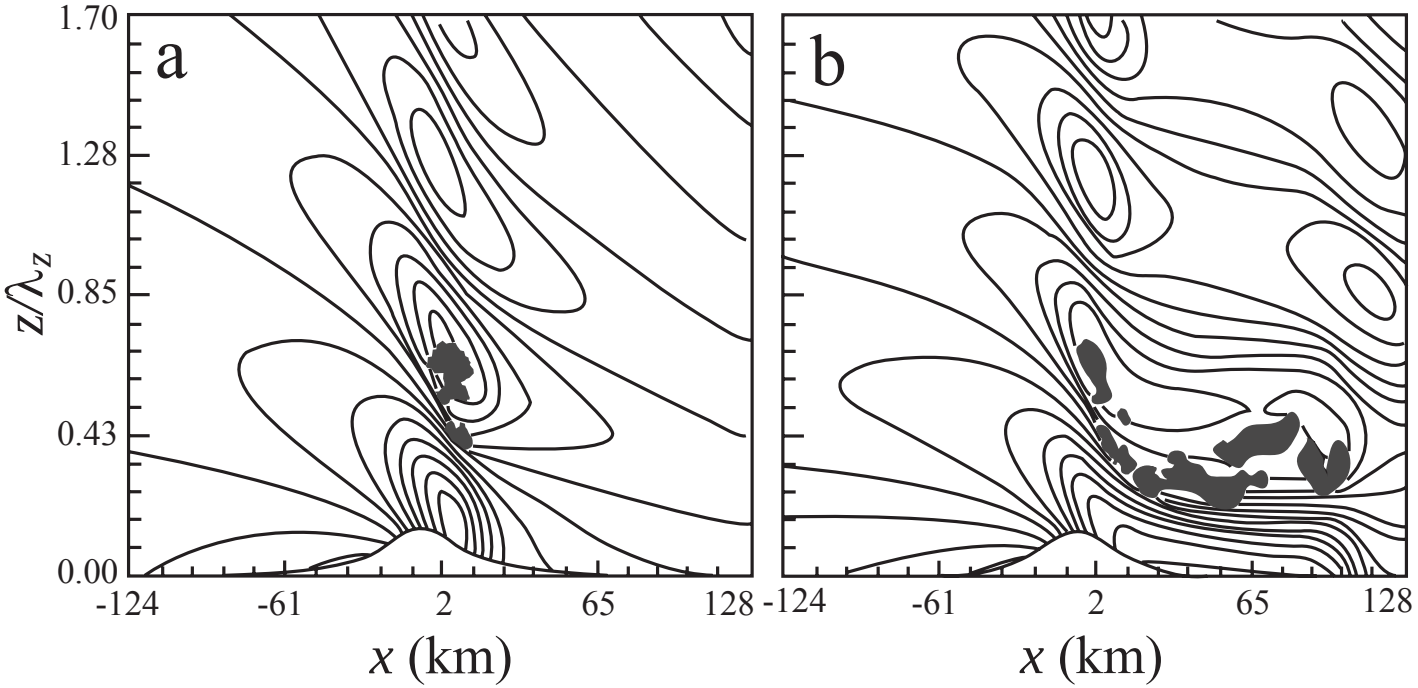

Wave ducting as revealed by the time evolution of horizontal wind speeds and regions of local $Ri < 0.25$ (shaded) for a flow with uniform wind and constant static stability over a mountain ridge at $Ut/a =$ (a) 12.6, and (d) 50.4. The Froude number of the uniform basic wind is 1.0. (Adapted after Wang and Lin 1999)

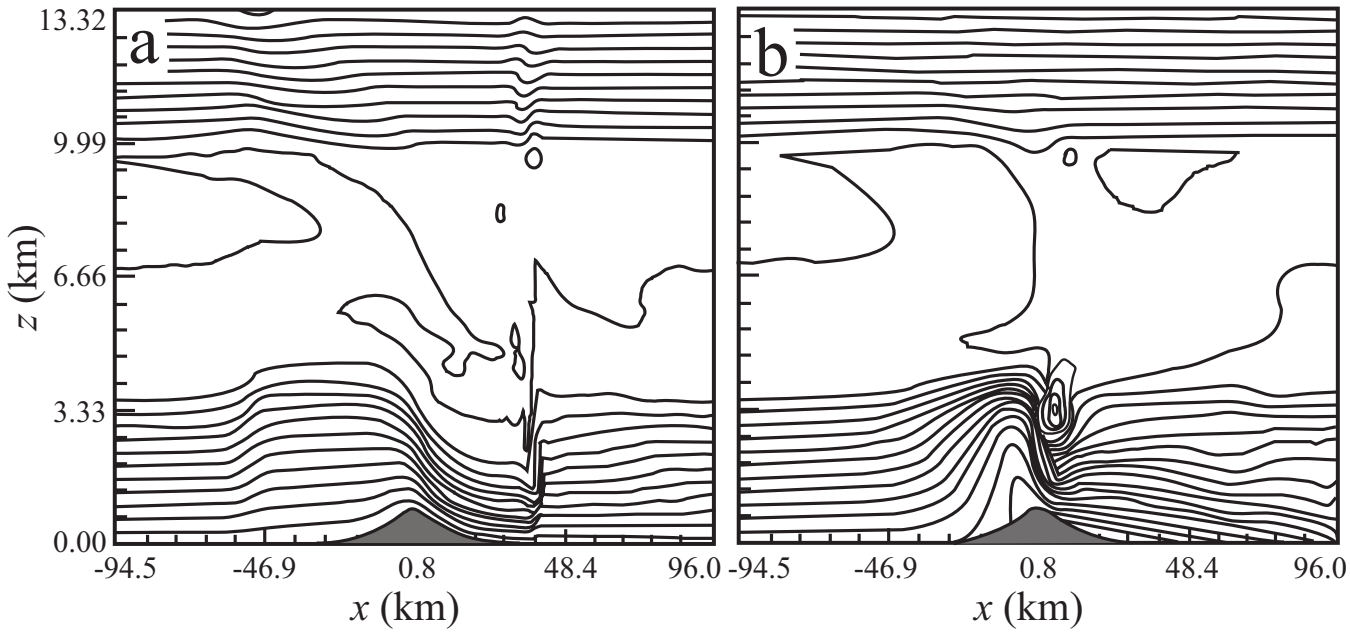

Effects of nonlinearity on the development of severe downslope winds: (a) Potential temperature field from nonlinear numerical simulations for a basic flow with $Ri = 0.1$ and $F = 2.0$; (b) Same as (a) except from linear numerical simulations. The contour interval is 1 K in both (a) and (b). (Adapted after Wang and Lin 1999)

Wave breaking occurs when waves reach large enough amplitudes.

When wave breaking occurs, it induces a critical level in the shear layer with low *Ri* and thus establishes a flow configuration favorable for *wave ducting* and *resonant amplification* in the lower uniform flow layer.

Hydraulic jump theory

HYDRAULIC JUMPS IN THE KITCHEN

The above image depicts a hydraulic jump in a "kitchen sink", which shows a very rapid change in the flow depth across the jump.

Around the place where the tap water hits the sink, you will see a smooth looking flow pattern. A little further away, you will see a sudden 'jump' in the water level. This is a hydraulic jump.

See an interesting animation at http://en.wikipedia.org/wiki/Hydraulic_jump.

A hydraulic theory was proposed to explain the development of severe downslope winds based on the similarity of flow configurations of severe downslope windstorms and finite-depth, homogeneous flow over a mountain ridge, (Smith 1985)

The hydraulic theory attributes the high-drag (severe-wind) state to the interaction between a smoothly stratified flow and the deep, well-mixed, turbulent "dead" region above the lee slope in the middle troposphere.

When a high-drag state develops, a *dividing streamline* encompasses this well-mixed region of uniform density (ρ_c in next figure).

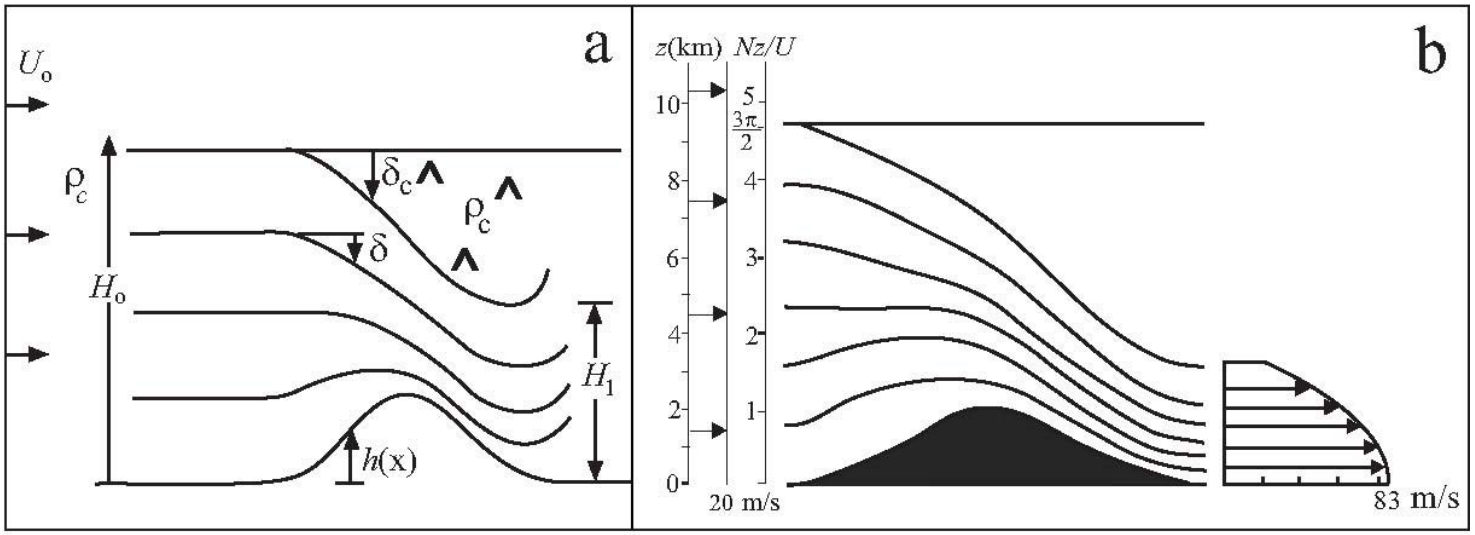

A severe downslope windstorm simulated by a hydraulic theory. (a) Schematic of an idealized high-drag state flow configuration. A certain critical streamline divides and encompasses a region of uniform density (ρ_c), which is called dividing streamline. (b) An example of transitional flow over a mountain.

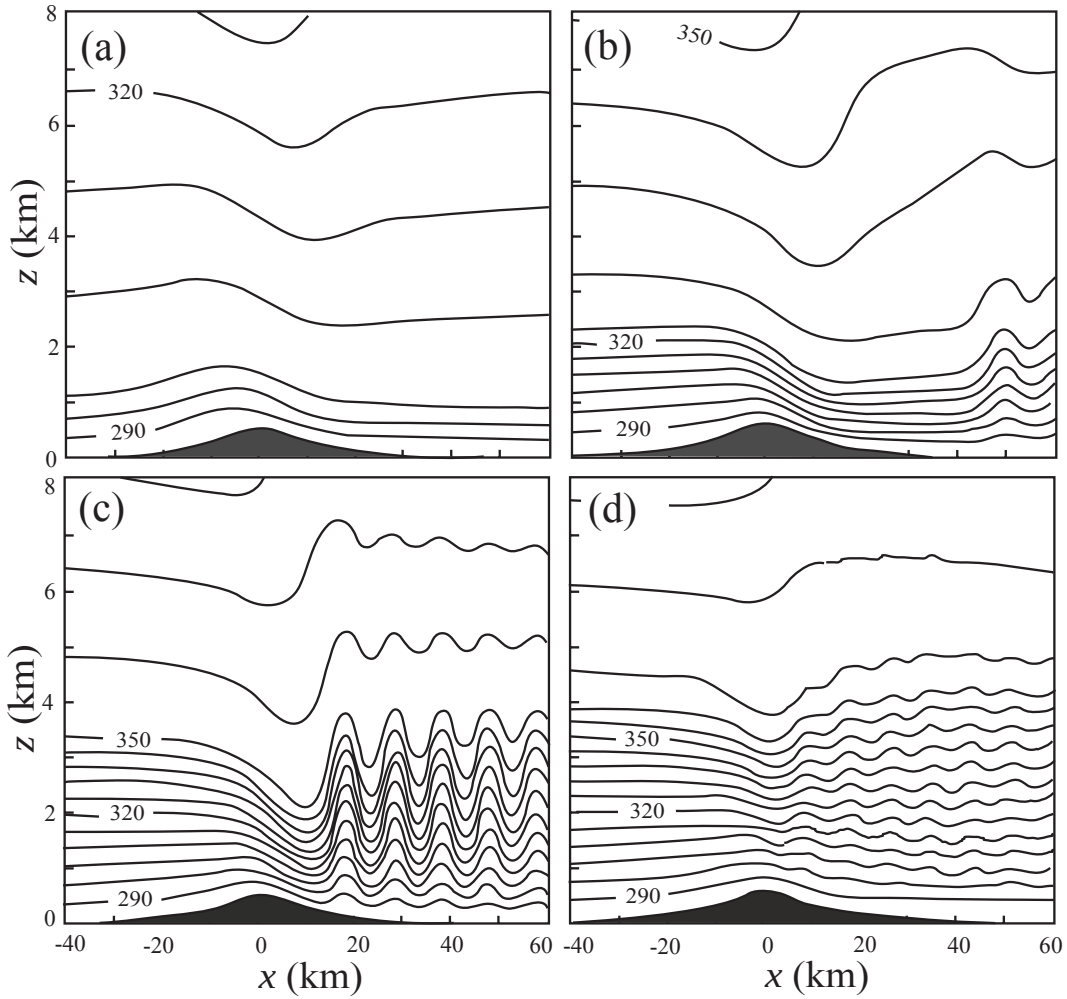

The dependence of high-drag states on the lower-layer depth, in the two-layer model (with different *N*), as revealed by the isentropes for airflow in a two-layer atmosphere at $Ut/a = 25$, when $N_1 h/U = 0.5$, where N_1 is the Brunt-Vaisala frequency of the lower layer, and the depth of the lowest, most stable layer (U/N_1) is: (a) 1, (b) 2.5, (c) 3.5, and (d) 4. The lower layer resembles: (a) supercritical flow, (b) a propagating hydraulic jump, (c) a stationary jump, and (d) subcritical flow. (After Durran 1986a)

Flows over three-dimensional mountains

Although the two-dimensional mountain wave theories helped explain some important flow phenomena generated by infinitely long ridges, such as upward propagating mountains waves, lee waves, wave overturning and breaking, and severe downslope winds, in reality most of the mountains are of three-dimensional, complex form.

The basic dynamics of flow over complex terrain can be understood by considering flow over an idealized, three-dimensional, isolated mountain.

We will look at a couple of phenomena associated with 3D mountains.

Trapped lee waves **behind a 3D mountain:**

As in the two-dimensional mountain wave problem, a rapid decrease of the Scorer parameter with height leads to the formation of *trapped lee waves*. The formation of three-dimensional trapped lee waves is similar to that of ***Kelvin ship waves*** over the water surface.

Next figure shows an example of the cloud streets associated with three-dimensional trapped lee waves produced by flow past a mountainous island. The wave pattern is generally contained within a wedge with the apex at the mountain.

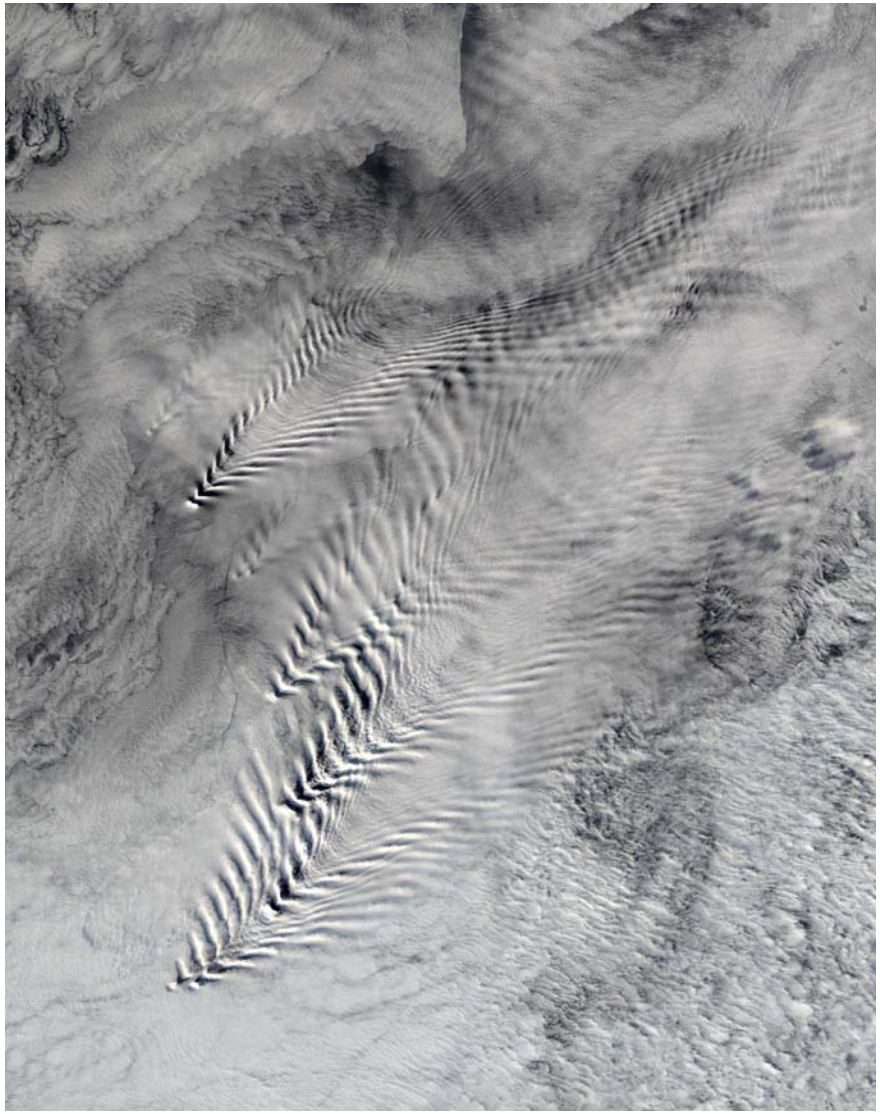

Satellite imagery showing hree-dimensional trapped lee waves induced by the South Sandwich Islands in southern Atlantic Ocean on September 18, 2003. The wave pattern is similar to that of the ship waves.

The three-dimensional trapped lee waves are composed by *transverse waves* and *diverging waves*.

The transverse waves lie approximately perpendicular to the flow direction, and are formed by waves attempting to propagate against the basic flow but that have been advected to the lee.

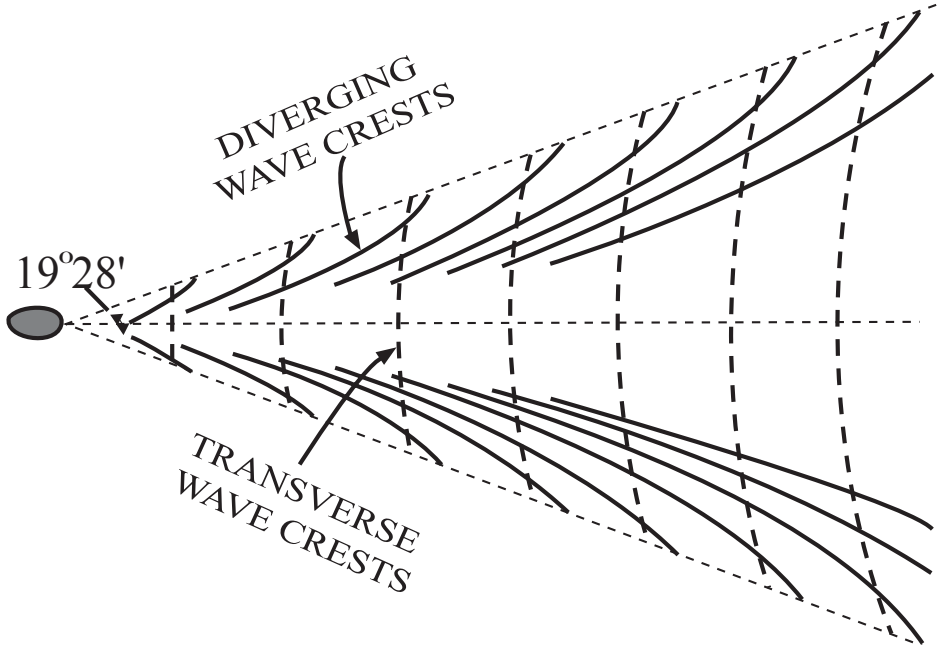

Schematic of transverse (bold-dashed) and diverging (solid) phase lines for a classical deep water ship wave. (Adapted after Sharman and Wurtele 1983)

The formation mechanism of transverse waves is the same as that of the two-dimensional trapped lee waves.

Unlike the transverse waves, the diverging waves attempt to propagate laterally away from the mountain and have been advected to the lee. Also, the diverging waves have crests that meet the incoming flow at a rather shallow angle.

When the *wake flow* in which the lee vortices are embedded becomes unstable, the vortices tend to shed downstream and form a ***von Kármán vortex street***.

A von Kármán vortex street is a repeating pattern of *alternate and swirling vortices* along the center line of the wake flow, and is named after the fluid dynamicist, Theodore von Kármán. This process is also known as ***vortex shedding*.**

A von Kármán vortex street that formed to the lee of the Guadalupe Island, off the coast of Mexico's Baja Peninsula, revealed by MISR images from June 11, 2000 detected by NASA satellite Terra. (From Visible Earth, NASA)